Emission-Color Control in Polymer Films by Memorized Fluorescence Solvatochromism in a New Class of Totally Organic Fluorescent Nanogel Particles

Nobuo Yamada, Hiroki Noguchi, Yoshifumi Orimoto, Yutaka Kuwahara, Makoto Takafuji, Shaheen Pathan, Reiko Oda, Almara Mahammadali Rahimli, Mahammadali Ahmed Ramazanov, Hirotaka Ihara

Emission-Color Control in Polymer Films by Memorized Fluorescence Solvatochromism in a New Class of Totally Organic Fluorescent Nanogel Particles

Nobuo Yamada,[a] Hiroki Noguchi,[a] Yoshifumi Orimoto,[a] Yutaka Kuwahara,[a] Makoto Takafuji,[a] Shaheen Pathan,[a, b] Reiko Oda,[b] Almara Mahammadali Rahimli,[c] Mahammadali Ahmed Ramazanov,[c] and Hirotaka Ihara*[a]

Abstract: In this work, a new class of totally organic fluorescent nanogel particles and their exceptionally specific behaviors based on their unique structures are introduced, which draws a sharp line from conventional fluorophore-doped and fluorophore-branched-type particles. The nanogel particles, the diameter of which could be controlled by adjusting reaction conditions, such as the solvent system, were spontaneously fabricated with a spherical shape by direct polymerization of non-heterocyclic aromatic compounds, such as 2,6-dihydroxyanthracene, 2,6-dihydroxynaphthalene, and 9,9-bis(4-hydroxyphenyl)fluorene with triazinane as the cross-linker. A fluorophoric moiety formed from a polymer main chain was realized in the particle, and consequently, the resultant content of the fluorophoric moiety was around 70–80 wt% per particle. The uniqueness and versatility of the particles can be emphasized by their good compatibility with various solvents due to their amphiphilic and ampholytic swelling properties, but also by their remarkable fluorescent solvatochromism in the dispersion state. Furthermore, these behaviors were preserved even in their polymer composite system. This study also demonstrates that various fluorescent polymer films can be fabricated with emission color control due to memorization of the solvatochromism phenomenon of the dispersed fluorescent nanoparticles.

Introduction

Nanosized fluorescent particles are now widely used in biochemistry, analytical chemistry, medicine, in fluorescence imaging,[1] optical signaling,[2] environment-sensitive probes,[2a,3] living-cell labeling,[1a,b,e,4] and immunochromatography.[5] Generally, a method of doping fluorescent materials into a nanosized carrier is widely known, and carriers such as colloidal silica,[6] magnetic particles[7] and graphene[8] have been used. Quantum dots mainly indicate nanoscale semiconductor crystals, and their bandgap can be adjusted depending on the size by the quantum effect. Quantum dots also have features, such as light emission in a wide wavelength region, high brightness, and long fluorescence lifetime,[1a,9] and are expected to be suitable for application in, for example., solar cells,[10] security tags[11] and lighting[12] and displays,[13] but there are many issues that still need to be solved, such as high cost, low stability, and poor dispersibility.

Against this background, the development of totally organic fluorescent particles not containing rare metals, highly toxic metals, and halogens has been desired. In general, there are two approaches to produce them: 1) doping the fluorescent dye in the above-mentioned carrier,[6–8] and 2) introducing a fluorescent chromophore into a side chain of a polymerizable monomer.[14] However, in these approaches, unavoidable limitations in terms of both the amount of dye that can be introduced in the carriers and the difficulty in preventing the elution of the dye from carriers are encountered. Furthermore, the introduced dye also presents issues that persist, such as a complex chemical structure and low stability.

This paper introduces an innovative method that essentially solves such problems (Scheme 1): totally organic nanoparticles composed of aromatic units (e.g., naphthalene, anthracene, fluorene, etc.) were produced upon polymerization and did not show the presence of heterocyclic structures. Thus, these nanoparticles were not prepared by doping with a fluorescent dye[1c,f,5a,7,12a,13d] or branching it synthetically to a polymer side chain,[3b,14,15] as for conventional fluorescent particles. In brief,

[a] *N. Yamada, Dr. H. Noguchi, Y. Orimoto, Dr. Y. Kuwahara, Prof. Dr. M. Takafuji, S. Pathan, Prof. Dr. H. Ihara*
Department of Applied Chemistry and Biochemistry, Kumamoto University
2-39-1 Kurokami, Chuo-ku, Kumamoto 860-8555 (Japan)
E-mail: ihara@kumamoto-u.ac.jp

[b] *S. Pathan, Dr. R. Oda*
Institute of Chemistry and Biology of Membranes and Nano-objects (UMR5248 CBMN), CNRS–Université de Bordeaux–Bordeaux INP
2 rue Robert Escarpit, Pessac 33607 (France)

[c] *A. Mahammadali Rahimli, Prof. Dr. M. Ahmed Ramazanov*
Physics Faculty, Baku State University
Z. Khalilov Street, 23 Baku, AZ1148 (Azerbaijan)

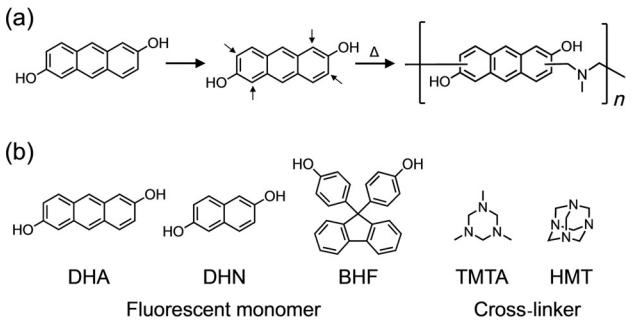

Scheme 1. One-pot fabrication of fluorescent gel particles. (a) Estimated reaction mechanism and structure of polymer. Small arrows on DHA indicate possible reaction sites with cross-linker. (b) Chemical structures of fluorescent monomers and cross-linkers. DHA: 2,6-dihydroxyanthracene, DHN: 2,6-dihydroxynaphthalene, BHF: 9,9-bis(4-hydroxyphenyl)fluorene, TMTA: 1,3,5-trimethyl-1,3,5-triazinane, HMT: hexamethylenetetramine.

this unique method involves a polymerization reaction by a one-pot process that produces spherical particles with diameters ranging from nano- to micrometers. The collection and purification of particles are extremely simple considering that no surfactant was used, but only one solvent, a small-molecule cross-linking agent, and the monomer were used. Furthermore, given that the fluorescent component is the main part of the particle that forms the polymer main chain without any carrier particles, the content of the fluorescent unit can be estimated as 70 wt% or more per particle. Because of this structure, there is no elution of the fluorescent unit. Also, due to the structural characteristics of the monomer and the cross-linking agent, the produced particles exhibit amphiphilic and amphoteric properties, so that they can be dispersed in various solvents and mixed with polymers without the use of surfactants. In addition, the fluorescent particles exhibit typical environmentally sensitive fluorescent solvatochromism.[16] The solvatochromism observed in a solution system can also be reproduced in a polymer composite system. Therefore, Stokes shifts can be controlled from the same fluorescent nanoparticles, making it possible to prepare optical films showing various luminescence colors, including white emission. This work describes the preparation method for such a new class of fluorescent nanoparticles, their unique fluorescence properties, and the preparation of luminescent films with controlled color emission.

Results and Discussion

Fundamental characterization of nanoparticles

The aspect in which this specific synthetic approach differs the most from the conventional method is that the spherical particles are prepared by directly polymerizing naphthalene, anthracene, fluorine, etc. (Scheme 1). The polymer particles were obtained by mixing a monomer with a cross-linker (listed in Scheme 1), and by heating at 150–200 °C in a microwave reactor for 3 min. The colors of the solution, in the case of the anthracene monomer, changed from light green to wine red, as shown in Figure S1 (Supporting Information). The collection and purification of the product were carried out by filtration with an appropriate membrane filter or by centrifugation and washing with THF or ethanol (good solvents). Table 1 summarizes the reaction conditions with the abbreviations of the obtained products. Figure 1 shows the TEM image of **Ant10-T_8W_2**, which was prepared from 2,6-dihydroxyanthracene (DHA) in a THF/water (8:2, *v*/*v*) mixture. The average diameter was determined to be around 30 nm by an image processing technique (A-zoukun, Asahi Kasei Engineering Co., Ltd., Kanagawa, Japan). As shown in Figure 1, similar spherical particles were also obtained by using 2,6-dihydroxynapthelene (DHN) and 9,9-bis(4-hydroxyphenyl)fluorene (BHF) as fluorescent monomers (listed in Scheme 1).

As shown in Table 1, the particle size of the products depended on the initial monomer concentration, the type of solvent, and the type of monomer. To investigate the aggregation mechanism producing nanoparticles, the size exclusion chromatography (SEC) of the remaining molecules after the polymerization reaction was carried out. As shown in Figure S2 (Supporting Information), the SEC chromatogram, in the case of **Ant10-T_8W_2**, detected several oligomers with $M_w < 9900$, but the higher-molecular-weight oligomers or polymers could not be found. This suggests that the solubility sharply decreases due to the formation of the oligomer, and the oligomers assembled like micelles to form a concentrated state. Moreover, it was confirmed that the obtained nanoparticles were well-dispersed in various solvents, such as water, methanol, ethanol, DMF, DMSO, ethyl acetate, THF, chloroform, and toluene, but also that they were insoluble in them.

Table 1. Reaction condition and average diameters of the products.

Particles	Monomer		Cross-linker		Solvent[a]	T[b]	Diameter[c]
	Kind	Conc. [mM]	Kind	Conc. [mM]		[°C]	[nm]
Ant10-T_8W_2	DHA	10	TMTA	10	T/W = 8:2	150	30
Ant20-T_8W_2	DHA	20	TMTA	20	T/W = 8:2	150	86
Ant30-T_8W_2	DHA	30	TMTA	30	T/W = 8:2	150	103
Ant10-D_8W_2	DHA	10	TMTA	10	D/W = 8:2	150	39
Ant20-D_8W_2	DHA	20	TMTA	20	D/W = 8:2	150	123
Ant10-E_8W_2	DHA	10	TMTA	10	E/W = 8:2	150	167
Naph30-E_5W_5	DHN	30	TMTA	30	E/W = 5:5	150	434
Flu30-E_5W_5	BHF	30	HMT	30	E/W = 5:5	200	315

[a] T: THF, D: DMF, E: ethanol, W: water. [b] The given temperature was maintained for 3 min in a microwave reactor. [c] Particle diameters were determined from TEM images by using the image analysis software (A-zoukun, Asahi Kasei Engineering Co., Ltd., Kanagawa, Japan).

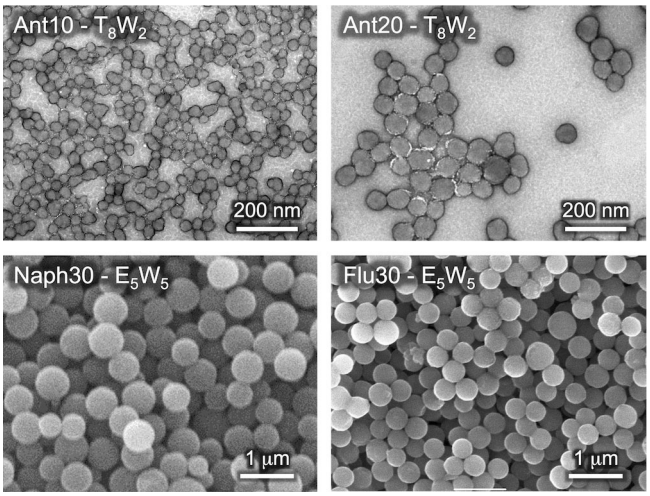

Figure 1. Electron micrographs of the particles obtained from various monomers. **Ant10-T_8W_2** and **Ant20-T_8W_2** were stained by using 1.0 wt% uranyl acetate for TEM analysis. **Naph30-E_5W_5** and **Flu30-E_5W_5** were coated by osmium oxide with the thickness of 5 nm for SEM.

These results indicate that the obtained particles have cross-linked structures. As a basis for estimating the formation of a cross-linked structure, it can be noted that there are multiple reaction sites in monomers. In the case of DHA (Scheme 1), there are four active points present at the C-1, C-3, C-5 and C-7 atoms and they are located next to the phenoxy group; thus, the cross-linker, -$CH_2N(CH_3)CH_2$- as the active species,[17] can be assumed to react with the anthracene ring at multiple positions. Table 2 shows the elemental analysis of the DHA-based nanoparticles. The measured values of carbon and nitrogen contents and C/N ratio are almost the same as the theoretical values calculated as the composition ratio of the anthracene component and -$CH_2N(CH_3)CH_2$- at 1:1 ratio (Scheme 1). It is reasonable to estimate that anthracene and -$CH_2N(CH_3)CH_2$- are alternately polymerized at 1:1, but considering that DHA contains four active sites, it seems that multi-cross-linking partially progresses. This presumed structure is in agreement with the fact that the produced nanoparticles are insoluble and swell in various solvents. Therefore, the particles produced should be classified as "gel" type one. The swelling property of the particles will be discussed later. Due to the complicated cross-linked structure, the exact chemical structure has not yet been identified, but in the FTIR spectra (Figure S3, Supporting Information), C–H stretching mode originating from -$CH_2N(CH_3)CH_2$- can be seen near 2900 cm^{-1}.

Table 2. Elemental analysis of DHA-based nanoparticles prepared by using various solvent systems.

Particles	C [%]	N [%]	H [%]	C/N	DHA content [%][b]
Ant10-T_8W_2	76.54	5.93	4.70	12.91	75.4
Ant10-D_8W_2	78.02	5.59	3.89	13.96	77.5
Ant10-E_8W_2	77.89	6.02	4.03	12.94	75.5
calcd[a]	76.96	5.28	5.70	14.58	79.2

[a] The calcd value was obtained based on 1:1 combination of DHA ($C_{14}H_8O_2$) and -$CH_2N(CH_3)CH_2$-. [b] The DHA content was calculated from the obtained C/N value.

The results of the elemental analysis indicate that the fluorescent component concentration remains high in the particle. For example, it was estimated that the anthracene contents were 75.4 wt% in the **Ant10-T_8W_2**, 77.5 wt% in the **Ant10-D_8W_2**, and 75.5 wt% in the **Ant10-E_8W_2** particles whereas the theoretical value in the 1:1 polymer was calculated as 79.2 wt%. This is the first example of nanoparticles in which the fluorescent component can be immobilized at the highest value. As described above, this cannot be realized in the conventional organic particles prepared by doping or side chain branching methods.

Dispersion in aqueous systems

Considering that all of the produced nanoparticles also exhibited good dispersibility in (good compatibility with) aqueous systems, it can be inferred that polar groups exist on the particle surface. By analyzing the reaction route shown in Scheme 1, it can be deduced that tertiary amine due to -$CH_2N(CH_3)CH_2$- as well as phenolic OH groups remain on the particle surface. In the FTIR spectrum (Figure S3, Supporting Information), the O–H stretching mode was observed around 3000 to 3500 cm^{-1}. To support these hypotheses, Figure 2a shows that **Ant10-T_8W_2** particles disperse in an aqueous solution in a wide range of pH values under soap-free conditions, exhibiting a yellow color in acidic aqueous solutions and a red-purple color in an alkaline aqueous solution. Figure 3 shows the pH dependence of the ζ potential. It can be seen that the **Ant10-T_8W_2** particles are positively and negatively charged under acidic and alkaline conditions, respectively. This means that **Ant_{10}-T_8W_2** are ampholytic as indicated by the equilibrium structures in Figure 3. Accordingly, the fluorescence color also varied with the pH value. As shown in Figure 2b, a yellow-green color (λ_{em} = 546 nm) under alkaline conditions and a red-orange color (λ_{em} = 620 nm) under acidic conditions were observed when the solutions were excited at 365 nm. This color

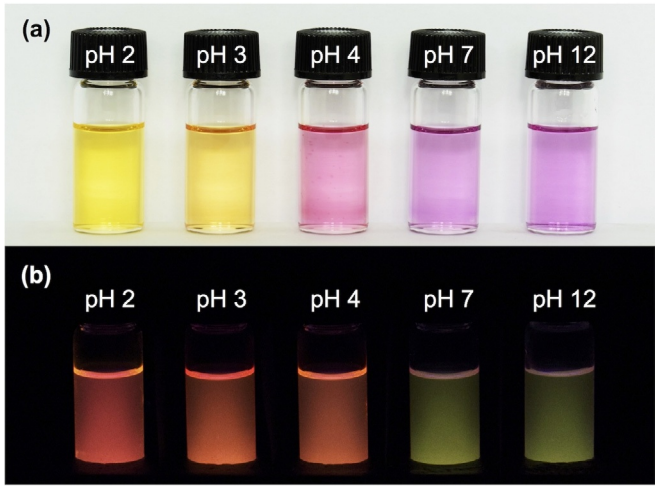

Figure 2. pH dependency of **Ant10-T_8W_2** dispersed in aqueous solutions (25 mg L^{-1}). (a) Under normal visible light, (b) excited at 365 nm.

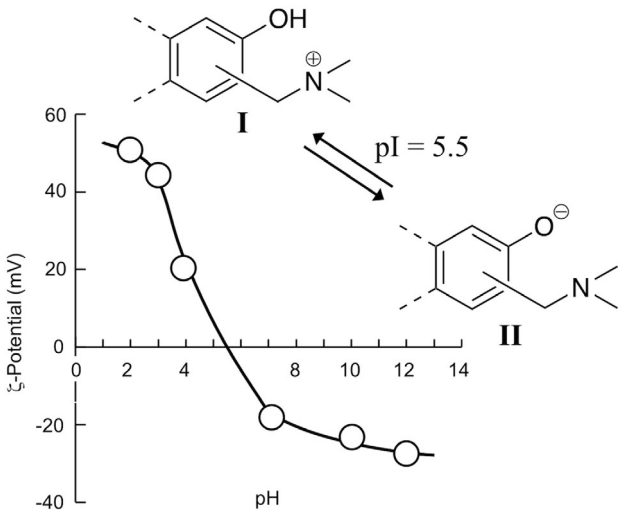

Figure 3. ζ-Potential curve of **Ant10-T_8W_2** in aqueous solutions at various pH values.

Table 3. Particle diameters and fluorescent properties of DHA and **Ant10-T_8W_2** in various solvents (5 mg L^{-1})

Solvent	Diameter[a] [nm]	Swelling degree[b]	Quantum yield (λ_{em}) Monomer[c]	Particle[d]
none	30	1.0	–	–
water, pH 2	75	2.5	21 (434)	12 (620)
water, pH 12	67	2.2	5 (513)	8 (546)
ethanol	83	2.8	17 (433)	20 (549)
DMF	241	8.0	22 (436)	108 (564)
DMSO	212	7.1	22 (440)	67 (563)
ethyl acetate	140	4.7	18 (434)	42 (553)
chloroform	180	6.0	20 (531)	92 (437)

[a] Diameters of the dried and dispersed particles were determined from TEM images and from DLS measurements, respectively. [b] Swelling degree values were calculated from the ratio between the diameters of dispersed particles and those of the dried ones. [c] Quantum yields of DHA (excited at 350 nm) were calculated as relative values for quinine sulphate in solutions, as shown for the detailed method in the Experimental Section. [d] QY values of the particles were calculated from values relative to DHA per anthracene ring.

change can be attributed to the structural change (pI = 5.5) between the states I and II indicated in Figure 3. The quantum yield values will be discussed later.

Fluorescent solvatochromism in organic solvents

As described above, the DHA-based nanoparticles have sufficient hydrophobicity to be dispersed in an organic solvent, and thus, they exhibit an amphiphilic nature: they can be dispersed in both water and organic solvents. Figure 4a shows that **Ant10-T_8W_2** is dispersed in various organic solvents to produce a clear solution. The high transparency can be the result of not only reduced agglomeration but also of the fact that the refractive index of the organic nanoparticles is close to that of the solvent, although strong light scattering is often observed in inorganic nanoparticles with a high refractive index. Table 3 contains the swelling degree of **Ant10-T_8W_2** in various solvents, which was determined from the ratio between the diameters of the wet state and the dry state. The results of the high swelling degree also explain the high transparency in organic solvents.

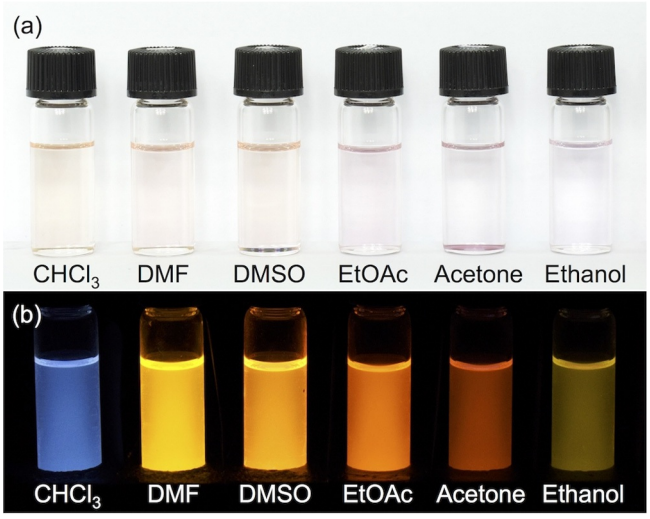

Figure 4. Ant10-T_8W_2 dispersed in various organic solvents (5 mg L^{-1}). (a) Under normal visible light, (b) excited at 365 nm.

Figure 4b shows the luminescence color of **Ant10-T_8W_2** dispersion in organic solvents upon irradiation with UV light of 365 nm. Interestingly, the luminescence color depended remarkably on the type of solvent. Therefore, we focused on the mixed solvent systems, that is, DMF/chloroform or ethyl acetate/chloroform, which had the most different luminescence colors, and the relationship between the composition ratio and luminescence color was investigated. As evident from Figure 5, the solvent change induced remarkable difference of the emission bands when the dispersions were excited at 350 nm: λ_{em} appeared at 437 nm in chloroform, but they were observed at longer wavelengths (by 116–127 nm), that is, at 564 and 553 nm in DMF and ethyl acetate, respectively. Such a fluorescence solvatochromism[16] is a typical phenomenon in which a Stokes shift appears due to the influence of, for examples, polarity and viscosity of the solvent in contact with the fluorescent unit. Given that a simple equilibrium phenomenon accompanying the solvent composition is observed in Figure 5, it can be concluded that the solvatochromism of **Ant10-T_8W_2** is based on the interaction that depends on the change in the microenvironment. It is probably related to the electron-donating property of -$CH_2N(CH_3)CH_2$-, which is a cross-linking unit and the formation of a hydrogen bond between the phenolic OH and the nitrogen atom.

Solvent-dependent fluorescence intensity

As clearly shown in Figure 4b, the fluorescent intensity is dependent on the solvent. Also, this can be explained as a result of the difference in the swelling degree. When the relative quantum yield (QY) to the monomer is plotted versus the swelling degree (Figure 6), it is revealed that a high QY is ob-

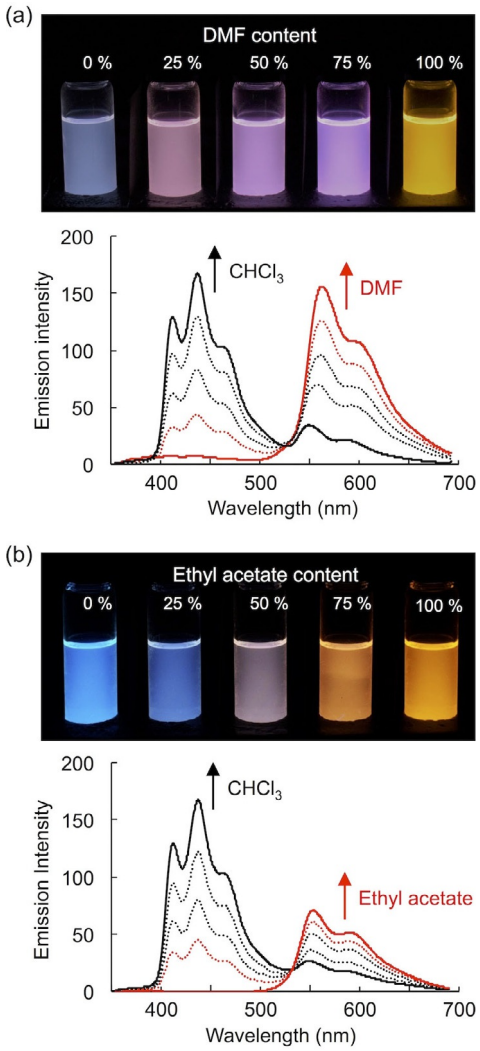

Figure 5. Fluorescent spectra and luminescence color of **Ant10-T_8W_2** in (a) chloroform/DMF and (b) chloroform/ethyl acetate mixtures.

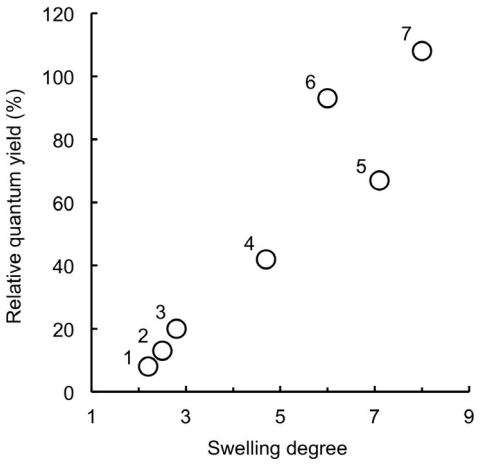

Figure 6. Correlation plots between swelling degree of polymer particle and relative quantum yield of **Ant10-T_8W_2** to DHA in various solvents. 1) Water (pH 12), 2) water (pH 2), 3) ethanol, 4) ethyl acetate, 5) DMSO, 6) chloroform, 7) DMF.

served for a high swelling degree. For example, the highest QY (108%) was observed for the highest swelling degree (8.0) in DMF, and the lowest QY (0.4–12) was observed in water, in which the swelling degree was in the range 2.2–2.5. This suggests that the swelling of the nanoparticles promotes the isolation of the polymer main chain, which is the luminescent component, and the luminescence efficiency becomes similar to that of the monomer as the isolation progresses. However, the relative QY of **Ant10-T_8W_2** in DMF reached 108%, which was slightly higher than that in monomeric DHA. This is thought to be due to the fact that the fluorescent component is completely isolated in DMF and also because the -$CH_2N(CH_3)CH_2$- moiety can act as an auxochromic group for the anthracene moiety.

Alternatively, it is not easy to explain the complicated redshift in the DHA particles compared with the monomer. One of the possible explanation is considered by an aggregation effect among the anthracene moieties. However, dilution with good solvents, such as DMF, promoted the solvation of an anthracene moiety to increase the fluorescent intensity as shown in Table 3 and Figure 6, and therefore, an aggregation-induced redshift is not in agreement with our results. The other possible mechanism for the redshift can be induced by an electron-donating, auxochromic effect due to the substitution of -$CH_2N(CH_3)CH_2$- moiety onto the anthracene ring. However, the substitution positions as well as the number of the substituents per an anthracene ring could not be identified, whereas they were determined to occur at 2–4 positions according to the elemental analysis (Table 2). In addition, the -$CH_2N(CH_3)CH_2$- moiety can be a cause of ring expansion to expand π-conjugated structures.[17b,18] Therefore, it is reasonable why the DHA particles exhibit complicated absorption bands in the wide range up to 450 nm as well as the specific absorption around 575 nm. A more detailed discussion on the structure could be subject of further investigation in the future.

Controlled emission in polymer composite system by memorized fluorescence solvatochromism

Considering that DHA-based nanoparticles exhibited good compatibility and dispersity even in general polymers, transparent thin films could be easily produced by a soap-free process. Figure 7 shows a composite film when **Ant10-T_8W_2** particles are incorporated in poly(methyl methacrylate) (PMMA). There was no significant decrease in the transparency due to the addition of **Ant10-T_8W_2** (Figure S5, Supporting Information). This indicates that the dispersibility of **Ant10-T_8W_2** is high for PMMA and secondary aggregation has not occurred. Also, as shown in Figure 7, it can be seen that the light-emitting function is maintained even in the solid film. This is presumed to be due to the fact that the **Ant10-T_8W_2** particles have a high affinity towards the base polymer and form a composite while maintaining the swollen state.

Interestingly, fluorescence solvatochromism of **Ant10-T_8W_2** was also observed during polymer film preparation. When the film formation was compared between ethyl acetate and

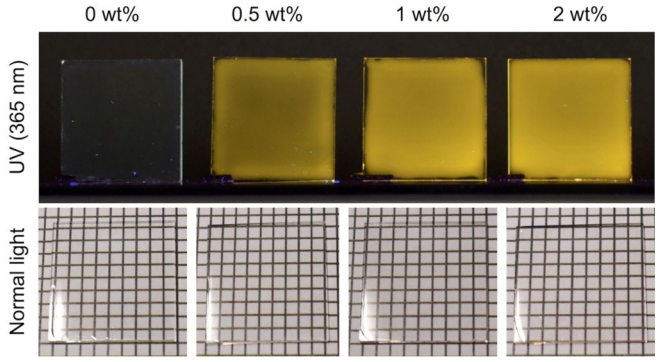

Figure 7. Images of **Ant10-T_8W_2**-containing PMMA films irradiated at 367 nm and under visible light. The composite films were prepared by casting on a glass plate from **Ant10-T_8W_2** and PMMA dispersed in ethyl acetate. Excitation wavelength: 365 nm.

chloroform systems, the emission color of the produced film corresponded to the emission color in the solution (Figure 8).

After sufficient drying, there was no change in the luminescence color even after being left at room temperature for one month. Thus, this is a good example exhibiting high stability of **Ant10-T_8W_2** but also the estimated state of OH···N interaction is assumed to be preserved in the polymer film, because it is difficult to consider the change in the luminescence color as due to residual solvent.

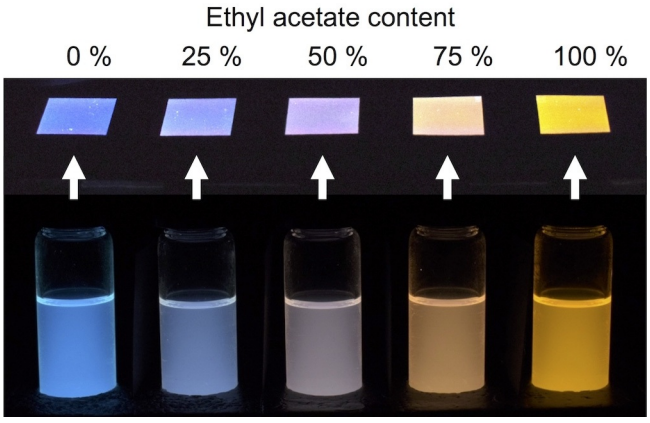

Figure 8. Fluorescence solvatochromism of **Ant10-T_8W_2** in the dispersion and in the solid state. **Ant10-T_8W_2** particles containing PMMA films were prepared by casting method on glass plate from **Ant10-T_8W_2** particle and PMMA dispersed in ethyl acetate and chloroform mixtures. The content of ethyl acetate was indicated on the top of Figure. Excitation wavelength: 365 nm.

Application to the other monomers

The versatility of our method can be emphasized by the fact that various monomers, such as naphthalene-based DHN and fluorene-based BHF derivatives, are applicable for this method as indicated in Table 1 and Figure 1. Figure 9 shows the fluorescence colors of the DHN- and BHF-based nanoparticles. Their fluorescent intensities were not enough strong, because excitation at 365 nm from the black light stage used in this study did not match their absorption bands. The stronger emissions from these particles were observed upon irradiation around their specific wavelengths (390–410 nm), as shown in Figures S6–S9 (Supporting Information).

Conclusions

In this paper, we have established a facile and quick method for creating totally organic fluorescent nanoparticles. The versatility of our method can be emphasized by good applicability for various monomers, such as anthracene-, naphthalene- and fluorine-based derivatives. The nanoparticles obtained showed distinct advantages over conventional fluorescent organic particles. 1) There is less elution of the fluorescent moiety from the particles because the fluorescent components form a polymer main chain. 2) Good dispersity was observed in both aqueous and non-aqueous solvents without addition of surfactants and surface modification. The amphiphilic properties impart compatible miscibility to various bulk polymers, which extends their possible optical applications. 3) Our organic nanoparticles showed typical fluorescence solvatochromism, which indicate their applicability as environmentally sensitive probe materials. By using this phenomenon, the controlled emission colors could be realized even in the polymer composite systems, and therefore, the fluorescent color of polymer films can be controlled by using these nanoparticles. This is the first example of the memorization of fluorescent solvatochromism in polymer systems, and it would expand their possible applications as optical films.

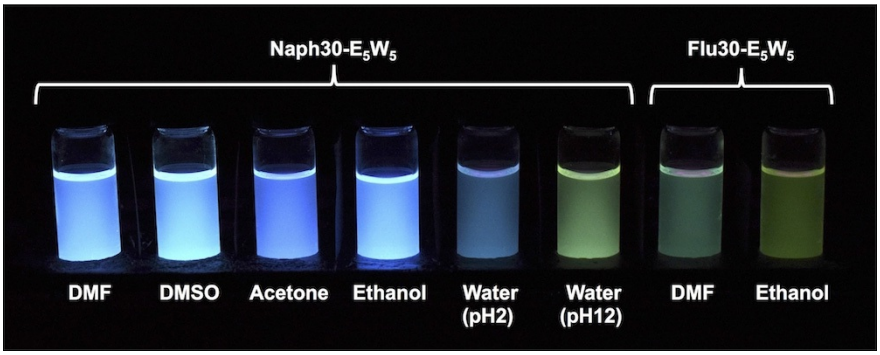

Figure 9. Fluorescent colors of **Naph30-E_5W_5** and **Flu30-E_5W_5** in various solvents (10 and 100 mg L^{-1}, respectively). Excitation wavelength: 365 nm.

Experimental Section

Chemicals

2,6-Dihydroxyanthracene, 2,6-dihydroxynaphthalene, 9,9′-bis(4-hydroxyphenyl)fluorene and 1,3,5-trimethyl-1,3,5-triazinane were purchased from Tokyo Chemical Industry Co., Ltd. Hexamethylenetetramine was purchased from Katayama Chemical Co., Ltd. Polymethylmethacrylate (PMMA) was purchased from Sigma–Aldrich Co. LLC. Reagent grade solvents and measurement grade solvents were purchased from Nacalai tesque, Inc. Polystyrene standard for Size Exclusion Chromatography (M_w = 500, 1010, 2500, 5870, 9490 and 17100) were purchased from Tosoh Corp.

Instruments

Preparation of polymer particles with a microwave reactor were carried out by using Monowave 300 (Anton Paar GmbH, Graz, Austria). Transmission electron microscopy (TEM) were performed with JEM-1400Plus (JEOL Ltd., Tokyo, Japan). The accelerating voltage of the TEM was 80 kV. Scanning electron microscope (SEM) were performed with Hitachi SU-8000 (Hitachi-Hightech Corp., Tokyo, Japan). The sample preparations were done by coating with 5 nm thin layers osmium tetroxide by using a osmium plasma coater OPC60A (Filgen Inc., Nagoya, Japan). The average diameter of polymer particles was determined by using the image analysis software (Asahi Kasei Engineering Co., Ltd., Kanagawa, Japan.) from the TEM and SEM images. Elemental analyses were carried out on a Yanaco CHN Corder MT-6 apparatus (Yanaco Co., Ltd., Kyoto, Japan). FTIR spectra were obtained by using a FT/IR-4100 (Jasco Co., Ltd., Tokyo, Japan) in the range of 4000–1000 cm^{-1}. UV/Vis absorption and fluorescence spectra were measured with V560 (Jasco Co., Ltd., Tokyo, Japan) and FP-6500 (Jasco Co., Ltd., Tokyo, Japan), respectively. ζ-potential and average particles diameter in dispersion states were performed with a Zetasizer nano ZS (Malvern Instruments Ltd., Worcestershire, UK) at 25 °C. Size exclusion chromatography (SEC) was carried out by using a PU-4180 pump (Jasco Co., Ltd., Tokyo, Japan) with a Reodyne Model 7725 injector, and a MD-4010UV-vis photodiode array detector (Jasco Co., Ltd., Tokyo, Japan) was used for the detection of samples. The column temperature was maintained by using CO-4060 column oven (Jasco Co., Ltd., Tokyo, Japan). A personal computer connected to the detector and pump, with the ChromNAV (version 1.17) software, was used for system control and data analysis. Shodex KF803 (Showa Denko K.K., Tokyo, Japan) was used as the SEC column.

Calculation of quantum yields

The quantum yield (QY) was calculated from the UV absorbance and the area of fluorescence spectra according to the following equation:[15c,19]

$$QY = QY_{st} \frac{I_x A_{st}}{I_{st} A_x} \left(\frac{n_x}{n_{st}} \right)^2$$

in which the subscript "x" designates the samples, the subscript "st" designates quinine sulfate, "QY" stands for quantum yield, "*I*" is the integral value of the fluorescence spectrum, "*A*" is the absorbance, and "*n*" is the refractive index of the solvent. Quinine sulfate (QY: 54%) as a measurement standard was dissolved in aq. 0.1 M H_2SO_4 (refractive index: 1.33). To minimize reabsorption effects of quinine sulphate, the absorbance of the individual solution was kept below 0.10 at the excitation wavelength (350 nm).

Preparation of anthracene-based nanoparticles

A typical synthetic procedure is the following. 2,6-Dihydroxyanthracene (42.0 mg, 0.20 mmol) and 1,3,5-trimethyl-1,3,5-triazinane (25.8 mg, 0.20 mmol) were dissolved in 20 mL of a THF/water mixed solvent (8:2). The mixture was placed into a 30 mL glass vessel, and then heated at 150 °C for 3 min with stirring (300 rpm) in the microwave reactor. The products were collected and washed by centrifugation (25000 rpm, 45 min) with THF. The precipitated product, **Ant10-T_8W_2** was dried in vacuo. **Ant10-T_8W_2** was obtained as a dark-purple powder. The other types of anthracene-based nanoparticles were prepared according to the similar procedure to **Ant10-T_8W_2** by changing the initial concentration and solvent system.

Preparation of Naph30-E_5W_5

2,6-Dihydroxynaphthalen (96.9 mg, 0.60 mmol) and 1,3,5-trimethyl-1,3,5-triazinane (77.5 mg, 0.60 mmol) were dissolved in 20 mL of an ethanol/water mixed solvent (5:5). The mixture was placed into a 30 mL glass vessel, and then heated at 150 °C for 3 min with stirring (300 rpm) in the microwave reactor. The resultant solution was filtered by using a cellulose acetate membrane filter (pore diameter = 0.2 μm) and the residual product, **Naph30-E_5W_5**, was collected. The product was washed with ethanol and dried in vacuo. **Naph30-E_5W_5** was obtained as a brown powder.

Preparation of Flu-E_5W_5

9,9′-Bis(4-hydroxyphenyl)fluorene (210.25 mg, 0.60 mmol) and hexamethylenetetramine (84.11 mg, 0.60 mmol) were dissolved in 20 mL of ethanol/water mixed solvent (5:5). The mixture was placed into a 30 mL glass vessel, and then heated at 200 °C for 30 min with stirring (300 rpm) in the microwave reactor. The resultant solution was filtered with cellulose acetate membrane filter (pore diameter = 0.2 μm) and the residual product, **Flu-E_5W_5** was collected. The product was washed with ethanol and dried in vacuo. **Flu-E_5W_5** was obtained as a yellow powder.

Preparation of polymer particles composite film

A typical preparation procedure is the following. **Ant10-T_8W_2** (2 mg) was dispersed in 20 mL of ethyl acetate. PMMA (100 mg) was separately dissolved in 10 mL ethyl acetate. 2 mL of the **Ant10-T_8W_2** solution and 2 mL of the PMMA solution were mixed, (**Ant10-T_8W_2**/PMMA = 0.2 mg:20 mg), then 300 μL of the mixture was casted on a glass plate (2.6 mm × 2.6 mm), and it was dried at room temperature. The obtained thin film on a glass contained 1 wt% of **Ant10-T_8W_2** for PMMA. The other **Ant10-T_8W_2**-containing PMMA films were prepared according to the similar method by changing the solvent and initial concentration.

Acknowledgements

This work was partially supported by a Grant-in-Aid for Scientific Research from MEXT of Japan, and from the Strategic International Collaborative Research Program (SICORP), "Molecular Technology" between JST in Japan and ANR in France.

Conflict of interest

The authors declare no conflict of interest.

Keywords: fluorescence · optical films · soap-free dispersions · solvatochromism · spherical particles

[1] a) W. C. W. Chan, S. M. Nie, *Science* **1998**, *281*, 2016 – 2018; b) P. Mitchell, *Nat. Biotechnol.* **2001**, *19*, 1013 – 1017; c) C. Y. Zhang, L. W. Johnson, *Angew. Chem. Int. Ed.* **2007**, *46*, 3482 – 3485; *Angew. Chem.* **2007**, *119*, 3552 – 3555; d) S. Fournier-Bidoz, T. L. Jennings, J. M. Klostranec, W. Fung, A. Rhee, D. Li, W. C. W. Chan, *Angew. Chem. Int. Ed.* **2008**, *47*, 5577 – 5581; *Angew. Chem.* **2008**, *30*, 5659 – 5663; e) B. Sun, M.-J. Sun, Z. Gu, Q.-D. Shen, S.-J. Jiang, Y. Xu, Y. Wang, *Macromolecules* **2010**, *43*, 10348 – 10354; f) Z. Wang, T. Qiu, L. Guo, J. Ye, L. He, X. Li, *React. Funct. Polym.* **2017**, *116*, 69 – 76.

[2] a) A. G. L. Olive, A. Del Guerzo, C. Schäfer, C. Belin, G. Raffy, C. Giansante, *J. Phys. Chem. C* **2010**, *114*, 10410 – 10416; b) J. Boekhoven, A. M. Brizard, M. C. A. Stuart, L. Florusse, G. Raff, A. Del Guerzoc, J. H. van Esch, *Chem. Sci.* **2016**, *7*, 6021 – 6031; c) T. Goto, Y. Okazaki, M. Ueki, Y. Kuwahara, M. Takafuji, R. Oda, H. Ihara, *Angew. Chem. Int. Ed.* **2017**, *56*, 2989 – 2993; *Angew. Chem.* **2017**, *129*, 3035 – 3039; d) H. Gao, P. Xue, J. Peng, L. Zhai, M. Sun, J. Suna, R. Lu, *New J. Chem.* **2019**, *43*, 77 – 84.

[3] a) K. Lugo, X. Miao, F. Rieke, L. Y. Lin, *Biomedical Opt. Exp.* **2012**, *3*, 447 – 454; b) V. V. Shvadchak, O. Kucherak, K. Afitska, D. Dziuba, D. A. Yushchenko, *Biochimica Biophysica Acta* **2017**, *1859*, 852 – 859; c) J. Rivnay, H. Wang, L. Fenno, K. Deisseroth, G. G. Malliaras, *Sci. Adv.* **2017**, *3*, e1601649.

[4] M. Bruchez Jr., M. Moronne, P. Gin, S. Weiss, A. P. Alivisatos, *Science* **1998**, *281*, 2013 – 2016.

[5] a) A. Sakurai, K. Takayama, N. Nomura, T. Munakata, N. Yamamoto, T. Tamura, J. Yamada, M. Hashimoto, K. Kuwahara, Y. Sakoda, Y. Suda, Y. Kobayashi, N. Sakaguchi, H. Kida, M. Kohara, F. Shibasaki, *PLoS One* **2013**, *8*, e76753; b) D. Wang, Z. Zhang, P. Liu, Q. Zhang, W. Zhang, *Sensors* **2016**, *16*, 1094.

[6] a) N. A. M. Verhaegh, A. Blaaderen, *Langmuir* **1994**, *10*, 1427 – 1438; b) J. E. Lee, N. Lee, H. Kim, J. Kim, S. H. Choi, J. H. Kim, T. Kim, I. C. Song, S. P. Park, W. K. Moon, T. Hyeon, *J. Am. Chem. Soc.* **2010**, *132*, 552 – 557; c) G. Stoica, I. C. Serrano, A. Figuerola, I. Ugarate, R. Pacios, E. Palomares, *Nanoscale* **2012**, *4*, 5409 – 5419.

[7] C. Kaewsaneha, P. Tangboriboonrat, D. Polpanich, A. Elaissari, *ACS Appl. Mater. Interfaces* **2015**, *7*, 23373 – 23386.

[8] C.-J. Hsieh, Y.-C. Chen, P.-Y. Hsieh, S.-R. Liu, S.-P. Wu, Y.-Z. Hsieh, H.-Y. Hsu, *ACS Appl. Mater. Interfaces* **2015**, *7*, 11467 – 11475.

[9] a) B. Ballou, B. C. Lagerholm, L. A. Ernst, M. P. Bruchez, A. S. Waggoner, *Bioconjugate Chem.* **2004**, *15*, 79 – 86.

[10] a) Y.-L. Lee, B.-M. Huang, H.-T. Chien, *Chem. Mater.* **2008**, *20*, 6903 – 6905; b) C. X. Guo, H. B. Yang, Z. M. Sheng, Z. S. Lu, Q. L. Song, C. M. Li, *Angew. Chem. Int. Ed.* **2010**, *49*, 3014 – 3017; *Angew. Chem.* **2010**, *122*, 3078 – 3081; c) H. C. Leventis, F. O'Mahony, J. Akhtar, M. Afzaal, P. O'Brien, S. A. Haque, *J. Am. Chem. Soc.* **2010**, *132*, 2743 – 2750; d) H. Jintoku, H. Ihara, *Chem. Commun.* **2012**, *48*, 1144 – 1146; e) H. Jintoku, M. Yamaguchi, M. Takafuji, H. Ihara, *Adv. Funct. Mater.* **2014**, *24*, 4105 – 4112; f) G. H. Carey, A. L. Abdelhady, Z. Ning, S. M. Thon, O. M. Bakr, E. H. Sargent, *Chem. Rev.* **2015**, *115*, 12732 – 12763; g) H. Tan, A. Jain, O. Voznyy, X. Lan, F. P. García de Arquer, J. Z. Fan, R. Quintero-Bermudez, M. Yuan, B. Zhang, Y. Zhao, F. Fan, P. Li, L. N. Quan, Y. Zhao, Z.-H. Lu, Z. Yang, S. Hoogland, E. H. Sargent, *Science* **2017**, *355*, 722 – 726; h) A. Kaewprajak, P. Kumnorkaew, T. Sagawa, *Org. Electron.* **2019**, *69*, 26 – 33.

[11] S. E.-S. Saeed, M. M. El-Molla, M. L. Hassan, E. Bakir, M. M. S. Abdel-Mottalebe, M. S. A. Abdel-Mottaleb, *Carbohydr. Polym.* **2014**, *99*, 817 – 824.

[12] a) S. Nizamoglu, T. Ozel, E. Sari, H. V. Demir, *Nanotechnology* **2007**, *18*, 065709; b) M. A. Schreuder, K. Xiao, I. N. Ivanov, S. M. Weiss, S. J. Rosenthal, *Nano Lett.* **2010**, *10*, 573 – 576.

[13] a) V. L. Colvin, M. C. Schlamp, A. P. Alivisatos, *Nature* **1994**, *370*, 354 – 357; b) S. Coe, W. K. Woo, M. Bawendi, V. Bulovic, *Nature* **2002**, *420*, 800; c) T.-H. Kim, K.-S. Cho, E. K. Lee, S. J. Lee, J. Chae, J. W. Kim, D. H. Kim, J.-Y. Kwon, G. Amaratunga, S. Y. Lee, B. L. Choi, Y. Kuk, J. M. Kim, K. Kim, *Nat. Photonics* **2011**, *5*, 176 – 182; d) Q. Zhou, Z. Bai, W. Lu, Y. Wang, B. Zou, H. Zhong, *Adv. Mater.* **2016**, *28*, 9163 – 9168.

[14] A. M. Breul, M. D. Hager, U. S. Schubert, *Chem. Soc. Rev.* **2013**, *42*, 5366 – 5407.

[15] a) F. Thielbeer, S. V. Chankeshwara, M. Bradley, *Biomacromolecules* **2011**, *12*, 4386 – 4391; b) X. Zhang, A. S. Shetty, S. A. Jenekhe, *Macromolecules* **1999**, *32*, 7422 – 7429; c) T. Liu, Y. Meng, X. Wang, H. Wang, X. Li, *RSC Adv.* **2013**, *3*, 8269 – 8275; d) M. Kasuya, T. Taniguchi, M. Kohri, K. Kishikawa, T. Nakahira, *Polymer* **2014**, *55*, 5080 – 5087.

[16] a) C. Reichardt, *Chem. Rev.* **1994**, *94*, 2319 – 2358; b) E. Yamaguchi, C. Wang, A. Fukazawa, M. Taki, Y. Sato, T. Sasaki, M. Ueda, N. Sasaki, T. Higashiyama, S. Yamaguchi, *Angew. Chem. Int. Ed.* **2015**, *54*, 4539 – 4543; *Angew. Chem.* **2015**, *127*, 4622 – 4626; c) A. S. Klymchenko, *Acc. Chem. Res.* **2017**, *50*, 366 – 375.

[17] a) T. Uyar, J. Hacaloglu, H. Ishida, *J. Appl. Polym. Sci.* **2013**, *127*, 3114 – 3123; b) A. Murakami, H. Noguchi, Y. Kuwahara, M. Takafuji, H. Ihara, *Chem. Lett.* **2017**, *46*, 680 – 682; c) M. N. Khan, Y. Orimoto, H. Ihara, *Chem. Commun.* **2018**, *54*, 13204 – 13207.

[18] N. Hano, M. Takafuji, H. Noguchi, H. Ihara, *ACS Appl. Nano Mater.* **2019**, *2*, 3597 – 3605.

[19] B. De, N. Karak, *RSC Adv.* **2013**, *3*, 8286 – 8290.

Manuscript received: March 17, 2019
Revised manuscript received: May 6, 2019
Accepted manuscript online: May 16, 2019
Version of record online: July 9, 2019